

# Photoinduced dynamically tunable terahertz metamaterial absorber

Liu Hongwei<sup>1</sup> Chen Qingchao<sup>1</sup> Sun Meiqi<sup>1</sup> Lü Junpeng<sup>2</sup>

(<sup>1</sup> School of Physics and Technology, Nanjing Normal University, Nanjing 210023, China)

(<sup>2</sup> School of Physics, Southeast University, Nanjing 211189, China)

**Abstract:** A photoexcited switchable single-band/dual-band terahertz metamaterial absorber with polarization-insensitive and wide-angle absorption is reported. The function switching is realized by modulating the conductivity of the photosensitive GaAs embedded in the resonator, and the surface currents at different GaAs conductivities are extracted to physically explain the absorption mechanism of the metamaterial absorber. The results show that the absorber can realize switching from dual-band absorption at 0.568 and 1.442 THz with 99.08% and 99.56% absorptivity, respectively, to a shift single-band absorption at 0.731 THz with 95.43% absorptivity. The device has an intensity modulation depth of 61.4% and a frequency tuning bandwidth of 60.6%. With these values, the device can be used to fabricate intensity modulators and frequency-selective absorbers in the terahertz band. In addition, the proposed absorber exhibits polarization-independent and wide-angle absorption for transverse electric (TE) and transverse magnetic (TM) polarization waves. The realization of tunable metamaterial absorbers offers opportunities for mature semiconductor technologies and potential applications in active terahertz modulators and switchers.

**Key words:** terahertz; metamaterial absorber; photoexcitation; dynamically tunable

**DOI:** 10.3969/j.issn.1003-7985.2024.02.005

Terahertz waves refer to electromagnetic waves with frequencies ranging from 0.1 to 10.0 THz. These waves have broad application prospects in imaging and modern technology, sensors, wireless communications, and other fields<sup>[1-4]</sup>. Electromagnetic metamaterials refer to a class of artificial composite structures or composite materials with extraordinary electromagnetic properties that natural materials do not possess. Terahertz metamate-

rials have received extensive attention because of their excellent penetrating ability, high bandwidth scalability, and high security. Currently, many new metamaterial devices in the terahertz range, such as absorbers<sup>[5-6]</sup>, filters<sup>[7]</sup>, modulators<sup>[8]</sup>, and switches<sup>[9]</sup>, have been proposed.

Since Landy et al.<sup>[5]</sup> first proposed metamaterial absorbers in 2008, metamaterial absorbers in multiple frequency bands have received extensive attention. Among these, metamaterial absorbers in the terahertz frequency band have become a hot research topic because of their potential applications in imaging, signal detection, and sensors<sup>[10-11]</sup>. However, after most metamaterial absorbers are successfully fabricated, their absorption strength and resonant frequency are fixed, which limits their practical application range to an extent. To solve this problem, researchers realized dynamic tuning of metamaterial absorber performance in the terahertz band by introducing phase change materials<sup>[12-13]</sup>, graphene<sup>[14]</sup>, liquid crystal materials<sup>[15]</sup>, photosensitive semiconductors<sup>[9, 16-20]</sup>, and other methods into the design.

For example, the temperature-control material, VO<sub>2</sub>, is used to realize the dynamic adjustment and control of the metamaterial absorber. By designing metamaterial absorbers with different structures, narrow-band and wide-band regulation can be achieved<sup>[12]</sup>. Switchable absorption from one broadband to another can also be achieved by stacking multilayered structures of VO<sub>2</sub><sup>[13]</sup>. The dynamic adjustment and control of metamaterial absorbers can be realized using electronically controlled materials. An absorber structure based on multilayered graphene strips of various sizes and cross-stacking of the media is designed. The Fermi energy of graphene is adjusted by changing the external voltage to realize switching between near-perfect absorption and reflection<sup>[14]</sup>. An external electric field is used to change the refractive index of the liquid crystal material embedded in the structural unit to realize the dynamic regulation of the metamaterial absorber<sup>[15]</sup>. Dynamic regulation of the metamaterial absorber can also be realized by irradiating the photosensitive semiconductor embedded in the metamaterial absorber using pump light. A light-regulated, single-frequency/dual-frequency switchable metamaterial absorber can be realized by embedding photosensitive semiconductor silicon into the gap of the open resonant ring<sup>[17]</sup>. By embedding pho-

**Received** 2024-01-04, **Revised** 2024-03-26.

**Biography:** Liu Hongwei (1986—), female, doctor, professor, phylhw@njnu.edu.cn.

**Foundation items:** The National Natural Science Foundation of China (No. T2222011, 62174026, 12274234), the National Key Research and Development Program of China (No. 2023YFB3611400, 2019YFA0308000), the Fundamental Research Funds for the Central Universities (No. 242023k30027).

**Citation:** Liu Hongwei, Chen Qingchao, Sun Meiqi, et al. Photoinduced dynamically tunable terahertz metamaterial absorber[J]. Journal of Southeast University (English Edition), 2024, 40(2): 148 – 154. DOI: 10.3969/j.issn.1003-7985.2024.02.005.

photosensitive silicon in different split rings of the combined resonator, a single-frequency/dual-frequency tunable terahertz absorber is realized<sup>[19]</sup>. Considering that GaAs has higher electron mobility, larger band gap, lower power consumption than Si<sup>[18, 21]</sup>, and light-controlled, ultrathin tunable metamaterial absorbers were fabricated using semiconductor GaAs patches<sup>[20]</sup>. Based on the response characteristics of different photosensitive semiconductor materials to different wavelengths of pump light, two photosensitive semiconductors can be embedded in the metamaterial absorber. An optically excited multifrequency terahertz switch based on a composite metamaterial structure is realized by embedding photosensitive silicon and germanium (Ge) in an open resonant ring<sup>[9]</sup>. The semiconductor gallium arsenide and germanium are embedded in a square ring-like structure to realize dynamic regulation of single-/dual-/triple-frequency absorption<sup>[16]</sup>.

Previous work has shown that phase change materials such as graphene, liquid crystal materials, and photosensitive semiconductors have great potential in the design of tunable terahertz absorbers. At a certain frequency range, most photoexcited dynamically tunable metamaterial absorbers can achieve only dynamic switching of several absorption states. Applications of such absorbers in intensity modulators and frequency-selective absorbers are lacking, which does not satisfy the increasing demand for practical applications<sup>[22]</sup>. In this paper, the conductivity of photosensitive GaAs embedded in a double-layer nested unit structure is modulated using the characteristic that the conductivity of photosensitive semiconductor materials can be regulated using an external pump light. In addition, dynamic regulation of single-frequency/dual-frequency absorption is realized. Through structural optimization, the intensity modulation depth and frequency tuning bandwidth are improved, and an excellent intensity modulator and frequency-selective absorber are made. In addition, by analyzing the surface current distribution and polarization-sensitive and oblique incidence characteristics of the absorber, the mechanism and absorption characteristics of the absorber-switching effect were investigated.

## 1 Structural Model

To confirm that the designed absorber has switchable absorption characteristics, the proposed structure is simulated using the microwave simulation software CST Microwave Studio 2018 based on finite integration technology. During simulation, set the  $x$ - and  $y$ -axes to the unit cell boundary condition and then set the  $z$ -axis to the open (add space) boundary condition. The electric field is along the  $x$ -axis direction, the magnetic field is along the  $y$ -axis direction, and the electromagnetic wave is incident on the absorber surface along the  $z$ -axis direction, as shown by the coordinates in Fig. 1(a). The absorption coefficient is calculated as follows. Absorption rate  $A(\omega)$  of the absorber can be obtained from the reflection coefficient

$S_{11}(\omega)$  and transmission coefficient  $S_{21}(\omega)$  extracted by simulation, namely

$$A(\omega) = 1 - R(\omega) - T(\omega) = 1 - |S_{11}(\omega)|^2 - |S_{21}(\omega)|^2 \quad (1)$$

where  $R(\omega)$  is the reflectivity;  $T(\omega)$  is the transmittance;  $\omega$  is the angular frequency. Because the bottom layer of the proposed structure uses a metallic film, electromagnetic waves cannot penetrate it. The thickness of the grounded metal plate in the structure is much larger than that of the skin depth of the incident wave in the metal film, so the transmittance,  $T(\omega)$ , is close to 0. Therefore, the absorption rate can be simplified as follows:

$$A(\omega) = 1 - R(\omega) = 1 - |S_{11}(\omega)|^2 \quad (2)$$

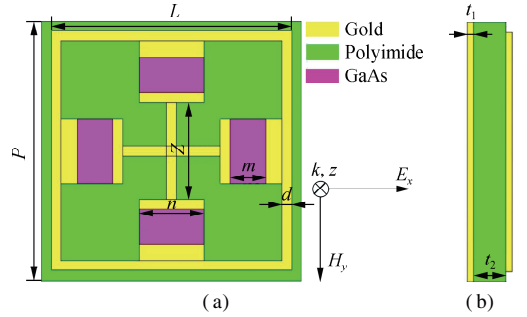


**Fig. 1** Metamaterial absorber cell structure. (a) Top view; (b) Side view

Figs. 1(a) and (b) show schematic diagrams of the unit structure of the resonator in the absorber. The resonator unit comprises a metal square ring and a cross metal wire structure. The photosensitive semiconductor GaAs is embedded in two metal structures. The GaAs block size  $m \times n$  at the gap between the inner and outer square rings is  $11 \mu\text{m} \times 20 \mu\text{m}$ . The bottom ground plane and the top metal pattern layer are both lossy gold films with a thickness of  $t_1 = 0.2 \mu\text{m}$  and a conductivity of  $4.561 \times 10^7 \text{ S/m}$ . The thickness of the photosensitive semiconductor gallium arsenide is the same as that of the gold film, and the relative dielectric of the photosensitive semiconductor is 12.94. The intermediate dielectric layer is made of polyimide material, its relative dielectric constant is 3.5, the loss tangent value is 0.008, and the thickness of the dielectric layer is  $t_2 = 7.5 \mu\text{m}$ . The cell structure size parameters are as follows:  $P = 80 \mu\text{m}$ ;  $L = 74 \mu\text{m}$ ;  $Z = 30 \mu\text{m}$ ;  $n = 20 \mu\text{m}$ ;  $d = 3 \mu\text{m}$ ; and  $m = 11 \mu\text{m}$ . The conductivity of the photosensitive semiconductor GaAs can be expressed as

$$\sigma_{\text{GaAs}} = \frac{i\varepsilon_0\omega_p^2}{\omega + i\gamma}$$

where  $\omega$  is the angular frequency of the incident light;  $\omega_p = \sqrt{n'e^2/(\varepsilon_0 m^*)}$  is the plasmon oscillation frequency;  $n'$  is the photogenerated carrier density;  $\varepsilon_0$  is the permittivity of free space;  $\gamma$  is the damping coefficient;  $m^*$  is the effective carrier mass<sup>[23]</sup>. Since the carrier density,

$n'$ , changes proportionally with the power of the pump light, the conductivity of GaAs can be regulated using an external pump light, and the dependence of the conductivity of GaAs on the pump power<sup>[19]</sup> can be fitted using the experimental parameters as follows:

$$\sigma_{\text{GaAs}} = 0.3204713I^3 - 15.89563I^2 + 778.914I + 91.16367$$

where  $I$  is the pump power, mW. In this paper, pump light with a wavelength of 800 nm is used to excite GaAs. When there is no light, the conductivity of GaAs is 100 S/m. With an increase in optical power, its conductivity can reach the order of  $10^5$ <sup>[18]</sup>; i. e., it gradually switches from the insulating state to the conduction state. In the conduction state, the resonant frequency and absorption intensity are changed so that the working state of the absorber can be regulated.

## 2 Results and Discussion

The decomposed structure of the absorber is shown in

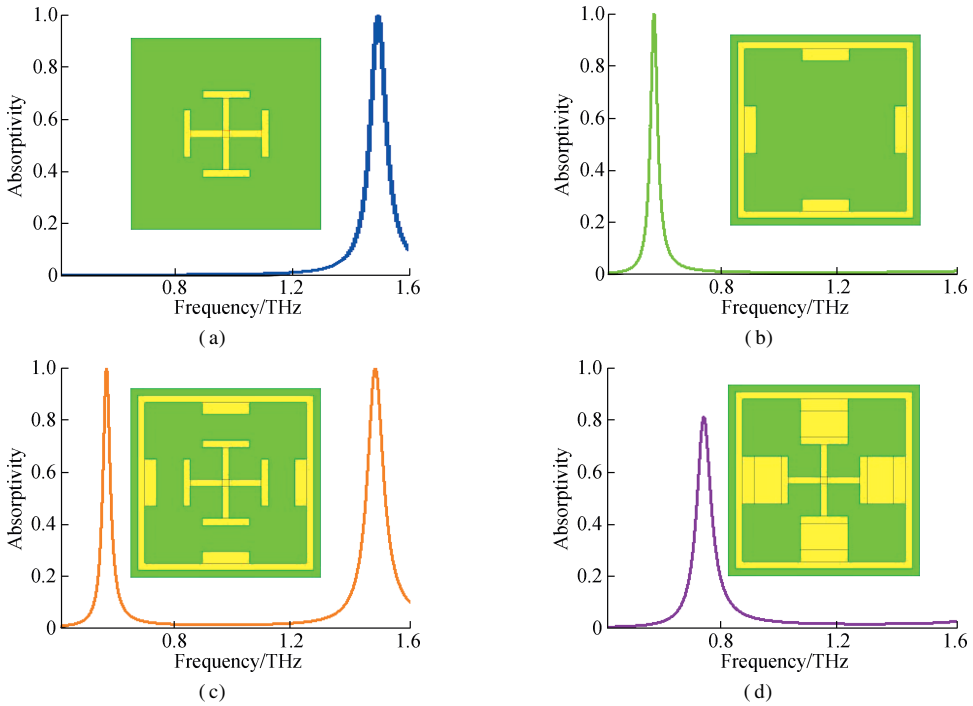


**Fig. 2** Decomposed structure and absorptivity curves of metamaterial absorbers. (a) Inner cross structure; (b) Inner raised square ring structure; (c) Two structures combined; (d) Two structures connected by a gold nugget

Based on the above decomposition structure, the dynamically tunable terahertz metamaterial absorber shown in Fig. 1 is designed by replacing the gold nugget in Fig. 2(d) with GaAs. When the surface of the absorber is vertically irradiated with pump light of wavelength 800 nm, the conductivity of GaAs gradually increases with the enhancement of illumination power, thus realizing the switching between the insulating and conducting states. Fig. 3 shows the simulated absorption spectra of GaAs absorbers with different conductivities. When there is no light pump irradiation, the corresponding GaAs conductivity is 100 S/m. Currently, the absorber forms two absorption peaks at 0.568 and 1.442 THz, and the

Fig. 2. Fig. 2(a) shows that when the top resonant unit is a cross-convex structure, the absorber resonates at 1.487 THz, and the absorption rate is 99.66%. It can be seen from Fig. 2(b) that when the top layer is a square ring structure with four inner protrusions, resonance occurs at 0.567 THz, forming an absorption peak with an absorption rate of 99.84%. Fig. 2(c) shows that the two substructures are combined to form a new resonant unit. The inner and outer structures can respond to incident electromagnetic waves. In addition, these structures can resonate at their respective resonance frequencies of 0.565 and 1.481 THz, forming a bimodal absorption peak with absorption rates of 99.77% and 99.83%. As shown in Fig. 2(d), the structures shown in Fig. 2(c) are further connected with gold nuggets; the connected structure can respond to electromagnetic waves as a whole; and it resonates at 0.737 THz, forming an absorption peak with an absorption rate of 80.90%.

absorption rates are 99.08% and 99.56%. With increasing pump power and conductivity of GaAs, the absorption rates of the two absorption peaks gradually decrease. The dual-frequency absorption is turned off when the conductivity of GaAs reaches a critical value of  $1.6 \times 10^4$  S/m, and the minimum absorption at 0.607 THz is 38.44%. As the conductivity of GaAs increases continuously, the absorption rate of the single-band absorber increases. When the conductivity of GaAs increases to  $2 \times 10^5$  S/m, a new absorption peak with an absorption rate of 95.43% is formed at 0.731 THz, completing the conversion from double-peak absorption to single-peak absorption.

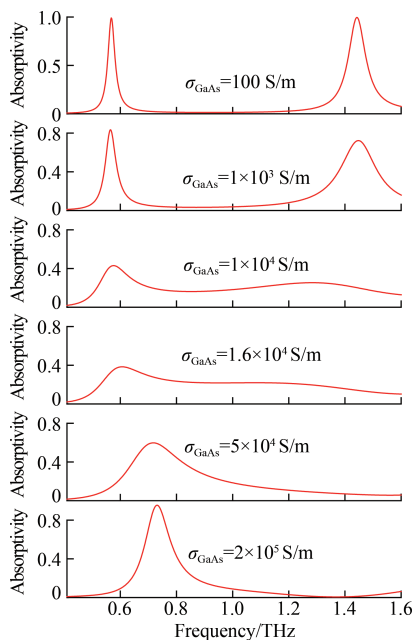


**Fig. 3** Absorption curves of dynamic changes under different GaAs conductivities

The intensity modulation depth,  $d$ , and frequency tuning bandwidth,  $b$ , of the metamaterial absorber can be defined as<sup>[24]</sup>

$$d = \frac{A_{\max} - A_{\min}}{A_{\max}}$$

$$b = \frac{f_1 - f_2}{f_1}$$

where  $A_{\max}$  and  $A_{\min}$  are the maximum and minimum absorption rates of the absorber;  $f_1$  and  $f_2$  are the highest and lowest frequencies corresponding to the absorption peak. The maximum modulation depth of the designed dynamic switchable dual-frequency absorber is calculated as 61.4%. The maximum frequency tuning bandwidth is 60.6%, which shows strong tunability. Therefore, the metamaterial absorber can be used as an intensity modulator and a frequency-selective absorber.

To further demonstrate the physical mechanism of the proposed switchable metamaterial absorber, we take the structure shown in Fig. 1 as an example to analyze the distribution frequency of the surface current during resonance, as shown in Fig. 4. Under irradiation with no pump light, the conductivity of GaAs is 100 S/m. The cross-convex structure and the square ring structure with four inner convex independently respond to the incident electromagnetic wave at two resonant frequencies to achieve dual-frequency absorption. Figs. 4(a) and (d) show the surface current distribution at the resonance frequency of 0.568 THz. For the absorption peak at 0.568 THz, the top surface current is mainly distributed in the outer structure; Figs. 4(b) and (e) show the surface current distribution at the resonance frequency of 1.442 THz. For the absorption peak at 1.442 THz, the top sur-

face current is mainly distributed in the inner structure and forms a reverse parallel current pair with the current of the metal base plate, which indicates that the two absorption peaks mainly come from the magnetic resonance response. When the conductivity of GaAs increases, the embedded GaAs connects the inner and outer resonant structures to form a new resonant structure. Therefore, the original two independent resonances at 0.568 and 1.442 THz can switch to a single response at the intermediate frequency of 0.731 THz. The surface current corresponding to 0.731 THz single-frequency absorption is shown in Figs. 4(c) and (f). The current is evenly distributed on the surface of the top resonant unit and the metal base plate, indicating that the new absorption peak originates from the common response of the inner and outer square rings to electromagnetic waves.

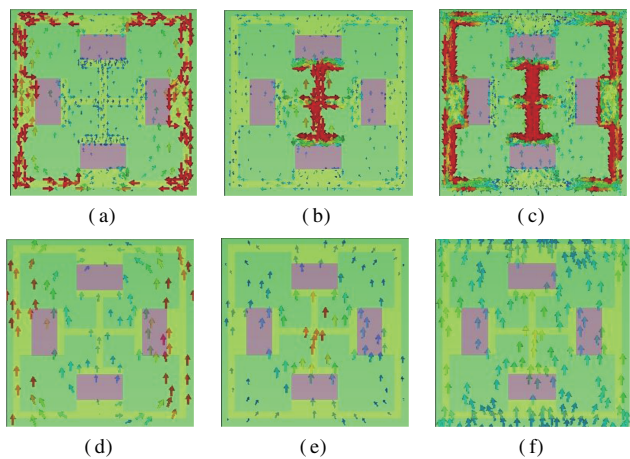


**Fig. 4** Surface current distribution under different GaAs conductivities. (a) Top surface current at 0.568 THz; (b) Top surface current at 1.442 THz; (c) Top surface current at 0.731 THz; (d) Bottom surface current at 0.568 THz; (e) Bottom surface current at 1.442 THz; (f) Bottom surface current at 0.731 THz

Furthermore, we investigate the polarization characteristics of the proposed structure by changing the polarization directions of the incident electromagnetic waves, as shown in Fig. 5. As the structure possesses quad-rotational symmetry, the absorptivity at a polarization angle of  $0^\circ$ - $45^\circ$  is considered. It is clear from Figs. 5(a) and (b) that in the dual-band mode without an optical pump, the absorption peaks at 0.568 and 1.442 THz remain unchanged for both transverse electric (TE) and transverse magnetic (TM) waves when the polarization angle changes from  $0^\circ$  to  $45^\circ$ . Similarly, in the single-band mode of the maximum pump power, the absorptivity is also unaffected by the polarization angles, as shown in Figs. 5(c) and (d). This means that the absorber is polarization-insensitive.

In practice, the electromagnetic waves are mostly incident on the absorber surfaces at different oblique angles. Wide-angle absorption is another important characteristic of absorbers. Fig. 6 presents the absorptivity at different incident angles for TE and TM polarization waves. It is observed from Figs. 6(a) and (b) that for the dual-band

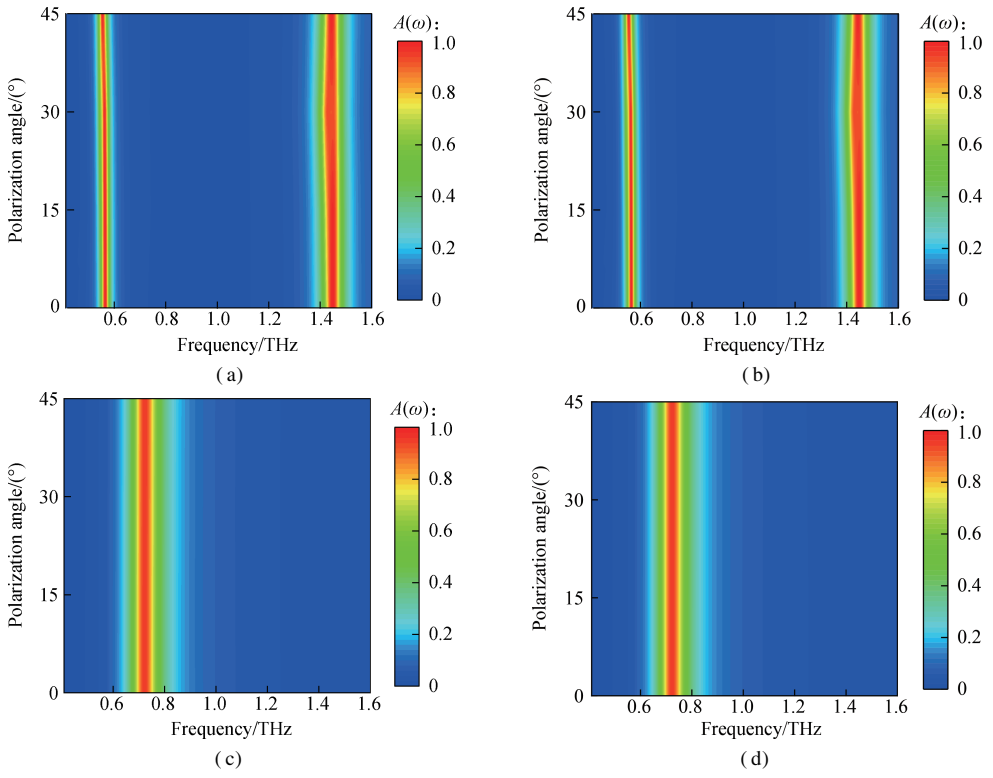


**Fig. 5** Absorptivity at different polarization angles  $\varphi$  under normal incident electromagnetic waves. (a) TE mode for no optical pump; (b) TM mode for no optical pump; (c) TE mode for maximum optical pump; (d) TM mode for maximum optical pump

mode at 0.568 and 1.442 THz, although the absorption peaks gradually decrease with the increase in incident angles, the absorptivity remains higher than 90% for the TE and TM polarization waves when the incident angle increases to 45°. However, in the TM mode, when the

incident angle increases, additional small absorption peaks are generated outside the operating frequency. These peaks are generated because of the parasitic resonance<sup>[25]</sup> in a certain part of the absorber with an increase in the incident angle.

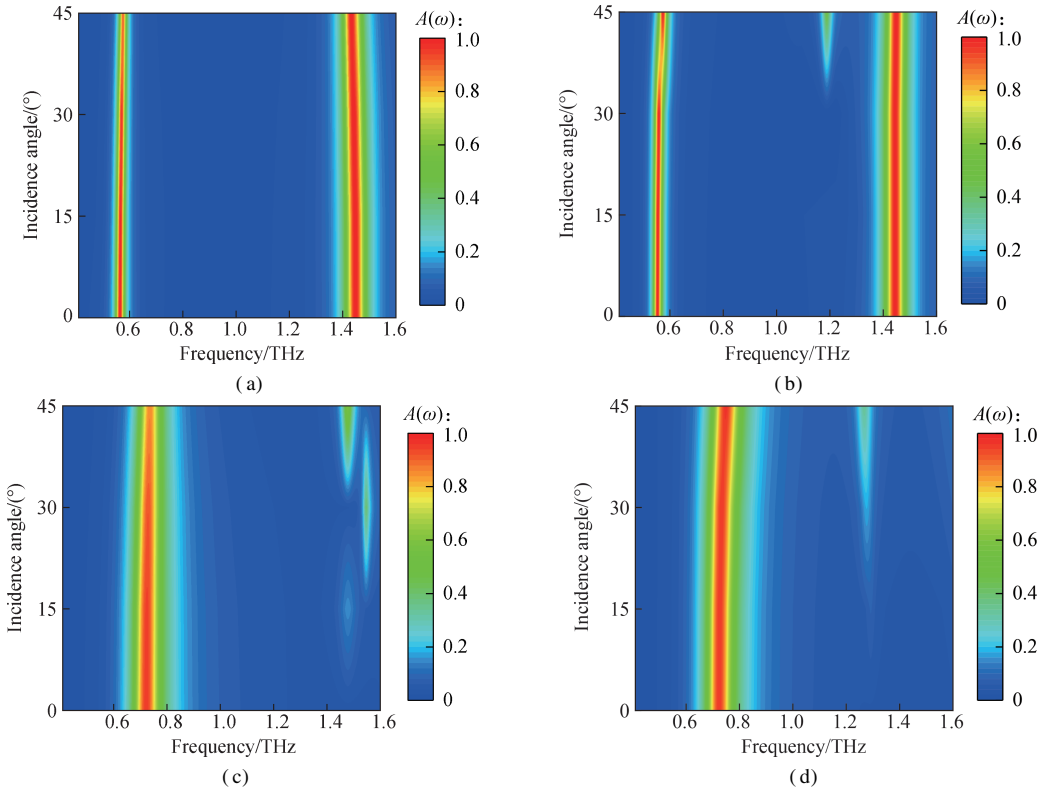


**Fig. 6** Absorptivity at different incidence angles  $\theta$  under normal incident electromagnetic waves. (a) TE mode for no optical pump; (b) TM mode for no optical pump; (c) TE mode for maximum optical pump; (d) TM mode for maximum optical pump

As shown in Figs. 6(c) and (d), for the single-band mode at 0.731 THz, the absorbance of the TE wave remains above 90% when the angle of incidence is increased to 45°, and the absorbance of the TM wave is less affected by the angle of incidence. For TE waves, the magnetic component along the  $y$ -axis gradually decreases, causing magnetic resonance to no longer be effectively excited when the incident angle increases up to a certain range. However, for TM waves, the magnetic component along the  $y$ -axis is unchanged with increasing incident angle, resulting in the absorptivity being almost unaffected by the incident angle. As shown in Fig. 6, with the increase in incident angles, additional absorption peaks are also observed for both the TE and TM modes, which can be caused by higher resonant modes in the proposed structure. Under normal incidence, multiple reflections and direct reflection from the top gold-patterned resonator destructively interfere, achieving near zero reflection and unity absorption at the resonant frequency. With an increase in the incident angle, these two reflections cannot be completely cancelled out, which results in a decreased absorption peak. The demonstrated results show that the proposed single-band/dual-band switchable metamaterial absorber can provide polarization-insensitive and wide-angle absorption for TE and TM waves.

### 3 Conclusions

1) The research results show that when there is no optical pumping, the photosensitive semiconductor GaAs is in an insulating state, and the proposed structure forms two near-perfect absorption peaks at 0.568 and 1.442 THz.

2) When a laser beam with a wavelength of 800 nm is used to excite GaAs in the on-state, the absorption state switches to a single peak absorption at 0.731 THz.

3) By using different illumination conditions to control the on-off state of the semiconductor GaAs, the proposed absorber can be arbitrarily switched between the single-frequency/dual-frequency perfect absorption states without changing the structure.

4) The metamaterial modulator has a maximum intensity modulation depth of 61.4% and a maximum frequency tuning bandwidth of 60.6%.

5) Because of the high symmetry of the designed absorber unit structure, the proposed switchable dual-frequency absorber has good polarization insensitivity and wide-angle absorption characteristics in both the TE and TM modes and has potential applications in modulators, sensors, and other fields.

### References

- [1] Federici J F, Schulkin B, Huang F, et al. THz imaging and sensing for security applications—Explosives, weapons and drugs[J]. *Semiconductor Science and Technology*, 2005, **20**(7): S266 – S280. DOI: 10.1088/0268-1242/20/7/018.
- [2] Jepsen P U, Cooke D G, Koch M. Terahertz spectroscopy and imaging—Modern techniques and applications[J]. *Laser & Photonics Reviews*, 2011, **5**(1): 124 – 166. DOI: 10.1002/lpor.201000011.
- [3] Liu X W, Liu H J, Sun Q B, et al. Metamaterial terahertz switch based on split-ring resonator embedded with photoconductive silicon [J]. *Applied Optics*, 2015, **54**(11): 3478 – 3483. DOI: 10.1364/AO.54.003478.
- [4] Zhao L. *Investigations on RF transceivers and related integrated circuits for a new generation broadband wireless internet*[D]. Nanjing: Southeast University, 2018. (in Chinese)
- [5] Landy N I, Sajuyigbe S, Mock J J, et al. Perfect metamaterial absorber [J]. *Physical Review Letters*, 2008, **100**(20): 207402. DOI: 10.1103/PhysRevLett.100.207402.
- [6] Wen Q Y, Zhang H W, Xie Y S, et al. Dual band terahertz metamaterial absorber: Design, fabrication, and characterization[J]. *Applied Physics Letters*, 2009, **95**(24): 241111. DOI: 10.1063/1.3276072.
- [7] Liu J J, Hong Z. Mechanically tunable dual frequency THz metamaterial filter [J]. *Optics Communications*, 2018, **426**: 598 – 601. DOI: 10.1016/j.optcom.2018.06.019.
- [8] Keshavarz A, Zakery A. A novel terahertz semiconductor metamaterial for slow light device and dual-band modulator applications[J]. *Plasmonics*, 2018, **13**(2): 459 – 466. DOI: 10.1007/s11468-017-0531-3.
- [9] Ji H Y, Zhang B, Wang G C, et al. Photo-excited multi-frequency terahertz switch based on a composite metamaterial structure [J]. *Optics Communications*, 2018, **412**: 37 – 40. DOI: 10.1016/j.optcom.2017.11.080.
- [10] Faruk A, Sabah C. Absorber and sensor applications of complimentary H-shaped fishnet metamaterial for sub-terahertz frequency region[J]. *Optik*, 2019, **177**: 64 – 70. DOI: 10.1016/j.ijleo.2018.09.145.
- [11] Yin S, Zhu J F, Xu W D, et al. High-performance terahertz wave absorbers made of silicon-based metamaterials [J]. *Applied Physics Letters*, 2015, **107**(7): 073903. DOI: 10.1063/1.4929151.
- [12] Song Z Y, Chen A P, Zhang J H. Terahertz switching between broadband absorption and narrowband absorption [J]. *Optics Express*, 2020, **28**(2): 2037 – 2044. DOI: 10.1364/OE.376085.
- [13] Zhao Y, Huang Q P, Cai H L, et al. A broadband and switchable VO<sub>2</sub>-based perfect absorber at the THz frequency[J]. *Optics Communications*, 2018, **426**: 443 – 449. DOI: 10.1016/j.optcom.2018.05.085.
- [14] Xu Z H, Wu D, Liu Y M, et al. Design of a tunable ultra-broadband terahertz absorber based on multiple layers of graphene ribbons [J]. *Nanoscale Research Letters*, 2018, **13**(1): 143. DOI: 10.1186/s11671-018-2552-z.
- [15] Shrekenhamer D, Chen W C, Padilla W J. Liquid crystal tunable metamaterial absorber [J]. *Physical Review*

- Letters*, 2013, **110**(17): 177403. DOI: 10.1103/physrevlett.110.177403.
- [16] Li D M, Yuan S, Yang R C, et al. Dynamical optical-controlled multi-state THz metamaterial absorber[J]. *Acta Optica Sinica*, 2020, **40**(8): 0816001. DOI: 10.3788/AOS202040.0816001. (in Chinese)
- [17] Cheng Y Z, Gong R Z, Cheng Z Z. A photoexcited broadband switchable metamaterial absorber with polarization-insensitive and wide-angle absorption for terahertz waves[J]. *Optics Communications*, 2016, **361**: 41–46. DOI: 10.1016/j.optcom.2015.10.031.
- [18] Yuan C, Zhao X L, Cao X L, et al. Optical control of terahertz nested split-ring resonators [J]. *Optical Engineering*, 2013, **52**(8): 087111. DOI: 10.1117/1.OE.52.8.087111.
- [19] Yuan S, Yang R C, Xu J P, et al. Photoexcited switchable single-/dual-band terahertz metamaterial absorber [J]. *Materials Research Express*, 2019, **6**(7): 075807. DOI: 10.1088/2053-1591/ab1962.
- [20] Zhao X G, Fan K B, Zhang J D, et al. Optically tunable metamaterial perfect absorber on highly flexible substrate [J]. *Sensors and Actuators A: Physical*, 2015, **231**: 74–80. DOI: 10.1016/j.sna.2015.02.040.
- [21] Pu Y Q, Shen H C, Tang F H, et al. Design of millimeter-wave reflective attenuators with capacitive compensation technique[J]. *Journal of Southeast University (English Edition)*, 2023, **39**(2): 153–160. DOI: 10.3969/j.issn.1003-7985.2023.02.006.
- [22] Xu O, Yang F, Sun Z L. Genetic algorithm design and measurement of sub-millimeter wave diagonal horn[J]. *Journal of Southeast University (Natural Science Edition)*, 2010, **40**(6): 1134–1139. DOI: 10.3969/j.issn.1001-0505.2010.06.002. (in Chinese)
- [23] Liu J X, Zhang K L, Liu X K, et al. Switchable metamaterial for enhancing and localizing electromagnetic field at terahertz band [J]. *Optics Express*, 2017, **25**(13): 13944. DOI: 10.1364/oe.25.013944.
- [24] Shen X P, Cui T J. Photoexcited broadband redshift switch and strength modulation of terahertz metamaterial absorber[J]. *Journal of Optics*, 2012, **14**(11): 114012. DOI: 10.1088/2040-8978/14/11/114012.
- [25] Yao G, Ling F R, Yue J, et al. Dual-band tunable perfect metamaterial absorber in the THz range[J]. *Optics Express*, 2016, **24**(2): 1518. DOI: 10.1364/oe.24.001518.

## 光致动态可调太赫兹超材料吸收器

刘宏微<sup>1</sup> 陈庆超<sup>1</sup> 孙美琪<sup>1</sup> 吕俊鹏<sup>2</sup>

(<sup>1</sup>南京师范大学物理科学与技术学院, 南京 210023)

(<sup>2</sup>东南大学物理学院, 南京 211189)

**摘要:**设计了一种具有偏振不敏感和广角吸收的光激发可切换单/双波段太赫兹超材料吸收器. 通过调制嵌入谐振器中的光敏砷化镓的电导率实现功能切换, 并提取不同砷化镓电导率下的表面电流, 对超材料吸收器的吸收机理进行了物理解释. 结果表明, 该吸收器可以实现从 0.568 和 1.442 THz 的双波段吸收(吸收率为 99.08% 和 99.56%) 到 0.731 THz 的单波段吸收(吸收率为 95.43%) 的切换. 该器件强度调制深度为 61.4%, 频率调谐带宽为 60.6%, 可制作太赫兹频段的强度调制器和频率选择吸收器. 此外, 所提出的吸收器对横电 (TE) 和横磁 (TM) 偏振波都具有与偏振无关的广角吸收. 可调谐超材料吸收器的实现为成熟的半导体技术以及有源太赫兹调制器和开关的潜在应用提供了机会.

**关键词:**太赫兹; 超材料吸收器; 光激发; 动态可调

**中图分类号:**O441; TB34